

Direct Metal Transfer between Periplasmic Proteins Identifies a Bacterial Copper Chaperone[†]

Ireena Bagai,[‡] Christopher Rensing,[§] Ninian J. Blackburn,^{*,||,⊥} and Megan M. McEvoy^{*,‡}

Department of Biochemistry and Molecular Biophysics and Department of Soil, Water, and Environmental Science, University of Arizona, Tucson, Arizona 85721, and Department of Environmental and Biomolecular Systems, Oregon Graduate Institute, School of Science and Engineering, Oregon Health and Sciences University, 20000 Northwest Walker Road, Beaverton, Oregon 97006-8921

Received August 28, 2008; Revised Manuscript Received September 23, 2008

ABSTRACT: Transition metals require exquisite handling within cells to ensure that cells are not harmed by an excess of free metal species. In Gram-negative bacteria, copper is required in only small amounts in the periplasm, not in the cytoplasm, so a key aspect of protection under excess metal conditions is to export copper from the periplasm. Additional protection could be conferred by a periplasmic chaperone to limit the free metal species prior to export. Using isothermal titration calorimetry, we have demonstrated that two periplasmic proteins, CusF and CusB, of the *Escherichia coli* Cu(I)/Ag(I) efflux system undergo a metal-dependent interaction. Through the development of a novel X-ray absorption spectroscopy approach using selenomethionine labeling to distinguish the metal sites of the two proteins, we have demonstrated transfer of Cu(I) occurs between CusF and CusB. The interaction between these proteins is highly specific, as a homologue of CusF with a 51% identical sequence and a similar affinity for metal, did not function in metal transfer. These experiments establish a metallochaperone activity for CusF in the periplasm of Gram-negative bacteria, serving to protect the periplasm from metal-mediated damage.

Transition metals such as copper are double-edged swords for living cells. Their redox capability is essential in numerous enzymatic processes (1). However, this ability to undergo redox transitions makes them commensurably toxic when present in excess of the required concentration. Additionally, the strong bonds that transition metals form with functional groups such as thiolates and imidazolium nitrogens in proteins contribute to their toxicity (2). Thus, the dual nature of transition metals continually challenges cells to maintain a delicate concentration balance within the

cellular milieu. An effective means of preventing the cytotoxic effects of copper is to keep it complexed (3). In other cells, most notably studied in yeast, cytoplasmic copper chaperone systems are useful for both sequestering and delivering copper to various proteins within the cell (4–10).

Escherichia coli cells, in common with the vast majority of bacterial cells, do not require copper for cytoplasmic enzymes but instead need copper for only periplasmic or inner membrane enzymes such as multicopper oxidases, Cu,Zn-superoxide dismutases, or the final enzyme of the respiratory chain, cytochrome *c* oxidase. Thus, while there is a need for some copper in the periplasm, the periplasm also appears to be the primary target of copper-mediated damage, making protective mechanisms necessary (11).

Efflux systems which remove excess copper are a common protective measure for the cells. The *E. coli* CusCFBA system is a Cu(I)/Ag(I) efflux system that pumps Cu(I) and Ag(I) to the extracellular space using the proton gradient across the inner membrane as an energy source (12). Three proteins in this system, CusA, CusB, and CusC, are members of the RND¹ (resistance, nodulation, division) or CBA type of efflux systems (13). The most-well studied members of

[†] We gratefully acknowledge the use of facilities at the Stanford Synchrotron Radiation Laboratory, which is supported by the National Institutes of Health Biomedical Research Technology Program, Division of Research Resources, and by the U.S. Department of Energy, Basic Energy Sciences (BES) and Office of Biological and Environmental Research (OBER). This work was supported by National Institutes of Health Grants GM54803 and PO1 GM067166 to N.J.B. and Grant GM079192 to M.M.M.

* To whom correspondence should be addressed. M.M.M.: e-mail, mcevoy@email.arizona.edu; phone, (520) 621-3489; fax, (520) 621-1697. N.J.B.: e-mail, ninian@ebs.ogi.edu; phone, (503) 748-1384; fax, (503) 748-1464.

[‡] Department of Biochemistry and Molecular Biophysics, University of Arizona.

[§] Department of Soil, Water, and Environmental Science, University of Arizona.

^{||} Oregon Health and Sciences University.

[⊥] Current address: Division of Environmental and Biomolecular Systems, Department of Science and Engineering, School of Medicine, Oregon Health and Sciences University, 20000 Northwest Walker Road, Beaverton, Oregon 97006-8921.

¹ Abbreviations: AHT, anhydrotetracycline; EXAFS, extended X-ray absorption fine structure; ITC, isothermal titration calorimetry; RND, resistance, nodulation, division; SDS–PAGE, sodium dodecyl sulfate–polyacrylamide gel electrophoresis; SeM–CusF, selenomethionine-labeled CusF; XAS, X-ray absorption spectroscopy.

this family have been those involved in multidrug resistance (e.g., AcrAB-TolC), and the metal resistance systems are thought to have many similarities in structure and function to these systems. CusA, CusB, and CusC are expected to form a protein complex that spans the inner and outer membranes. Pathways for substrate efflux have not been directly determined in these kinds of systems, but studies of multidrug resistance systems suggest substrate uptake is likely from the periplasmic space or potentially from within the inner membrane in the case of hydrophobic compounds (14, 15). In the Cus system, metal binding by the periplasmic protein CusB serves an essential role in Cus-mediated resistance (16), and thus, CusB could potentially provide a direct point of entry for metal substrates into the efflux complex. In monovalent metal resistance systems, there is a fourth component, CusF, which is a small periplasmic metal binding protein of unknown function. CusF could act as a metallochaperone to deliver metal to the Cus system for removal from the periplasm, or alternately, it could serve as a metal-dependent regulator of the CusCBA complex (17).

A chaperone for an efflux system could play a dual protective role through both sequestration of metal and enhancement of delivery of metal for subsequent export. In this work, we demonstrate specific and direct metal transfer between CusF and CusB, providing evidence for CusF as a metallochaperone. CusF could thus play a role in protecting the periplasmic compartment from metal-induced damage by both limiting the free copper in the periplasmic space and aiding in removal of copper from the cell.

MATERIALS AND METHODS

Protein Expression and Purification. The expression and purification of CusF and CusB in *E. coli* were performed as described previously (16, 17) except as noted below. For X-ray absorption spectroscopy (XAS) studies, selenomethionine-labeled CusF (SeM-CusF) was produced from *E. coli* BL21(λ DE3) cells containing the pASKIBA3/*cusF* plasmid grown in M9 minimal medium supplemented with L-selenomethionine, leucine, isoleucine, and valine at 50 mg/L and lysine, phenylalanine, and threonine at 100 mg/L (18). All the buffers used for the purification of SeM-CusF contained 10 mM dithiothreitol.

Plasmid pMG101 from *Salmonella typhimurium* was used to amplify the *silF* gene. The primers used for the PCR contained unique restriction sites at the 5' end (*Eco*RI) and 3' end (*Xho*I). After restriction enzyme digestion of the PCR product, it was ligated into the pASK-IBA3 (IBA) vector. The result was a construct, pASK-*silF*₈₋₉₄, encoding the SilF protein lacking the signal peptide sequence and the first seven residues at the N-terminus. The protein produced from this construct contains seven additional residues at the N-terminus encoded by the plasmid.

The pASK-*silF*₈₋₉₄ plasmid was transformed into *E. coli* BL21(λ DE3). Cells were grown in LB medium containing 100 μ g/mL ampicillin at 37 °C until an OD₆₀₀ of 0.6–1.0 was reached. Cells were induced with 200 μ g/L anhydrotetracycline (AHT) and grown at 30 °C for an additional 6–8 h. Cells were harvested by centrifugation and frozen at –20 °C. The cell pellet was thawed and resuspended in approximately 75 mL of 100 mM Tris (pH 8.0), 150 mM NaCl buffer per liter of cell culture. The procedure used for

processing of the cell pellet, including lysis and centrifugation, was the same as that used for the CusF and CusB purifications. The supernatant obtained from centrifugation of the cell lysate was dialyzed against 60 mM lactate (pH 3.5), 50 mM NaCl buffer. After three changes of dialysis buffer, the precipitated proteins were removed by centrifugation at 12000g, and the resulting supernatant was loaded onto a HighPrep 16/10 Sepharose Fast Flow cation exchange column (Amersham) equilibrated with lactate buffer used for dialysis. SilF was eluted using a linear gradient from 50 to 500 mM NaCl in 60 mM lactate buffer with a pH gradient from 3.5 to 5.0. Fractions containing SilF were identified using SDS–PAGE, combined, and concentrated to approximately 0.5 mL using Amicon concentrators with a 5 kDa molecular mass cutoff. The concentrated protein was applied to a S100 size exclusion column (Amersham) equilibrated with 100 mM phosphate (pH 8.0), 100 mM NaCl buffer. Aliquots of the fractions were run on SDS–polyacrylamide gels, and fractions judged to be >95% pure, as determined using Coomassie staining, were pooled and dialyzed in 50 mM cacodylate (pH 7.0) buffer. Proteins were concentrated as described above. Protein concentrations were determined using the BCA assay (Pierce Biotechnology).

Isothermal Titration Calorimetry (ITC). ITC measurements were performed on a Microcal (Northampton, MA) VP-ITC microcalorimeter, typically at 25 °C. To load proteins with Ag(I), a AgNO₃ solution in H₂O from a 100 \times stock was added at approximately twice the concentration of the protein, followed by dialysis in 50 mM cacodylate (pH 7.0) to remove excess Ag(I). Protein in either the apo or Ag(I)-bound state was concentrated using Amicon concentrators with a 5 kDa cutoff to the desired concentrations for the ITC experiments. The titrand and the titrant were thoroughly degassed in a ThermoVac apparatus (Microcal). For a titration experiment, approximately 1.5 mL of titrand protein was placed in a reaction cell and injected with the titrant protein over the course of 20 s. The first injection was 2 μ L, and all subsequent injections were 10 μ L. A total of 25 injections were made with 5 min intervals between each injection. The following titrations were performed: apo-CusF (375 μ M) into apo-CusB (20 μ M), Ag(I)-CusF (375 μ M) into apo-CusB (24 μ M), Ag(I)-CusF (375 μ M) into Ag(I)-CusB (23 μ M), and Ag(I)-CusB (142 μ M) into apo-CusF (17 μ M) (the concentrations are the protein concentrations of the starting material). To ensure adequate mixing of the two proteins, the reaction cell was continuously stirred at 300 rpm. The heat due to dilution, mechanical effects, and other nonspecific effects were identified by averaging the last three points of the titration and subtracting that value from all data points (27). No attempt was made at fitting these data to obtain binding affinities or stoichiometries, since the experiments are expected to be reflective of both protein–protein interactions and metal binding and/or release.

For ITC experiments with SilF, Ag(I)-bound protein where needed was prepared as described above for CusF and CusB, and the following titrations were performed: AgNO₃ (300 μ M) into apo-SilF (36 μ M), Ag(I)-SilF (170 μ M) into apo-CusB (21 μ M), Ag(I)-SilF (170 μ M) into apo-CusF (29 μ M), and Ag(I)-CusF (275 μ M) into apo-SilF (30 μ M). In each case, the buffer was 50 mM cacodylate (pH 7.0). As controls for all the ITC experiments, each protein was titrated into buffer, or buffer was titrated into each protein to determine

the heat changes due to protein dilution. For the titration of apo-SilF with AgNO_3 , a single-site binding model was fitted to the data using Origin (Microcal). The software uses a nonlinear least-squares algorithm and the concentrations of the titrant and the titrand to fit the enthalpy change per injection to an equilibrium binding equation. The binding enthalpy change (ΔH), association constant (K_a), and binding stoichiometry (n) were permitted to float during the least-squares minimization process and taken as the best-fit values.

Preparation of Samples for X-Ray Absorption Spectroscopy (XAS). CusB and SeM-CusF in 20 mM *N*-(2-acetamido)-2-aminoethanesulfonic acid (ACES) (pH 7.0) were purged with argon and then transferred to the anaerobic chamber. An ascorbate solution buffered at pH 7.0, which was prepared inside the anaerobic chamber, was added to the argon-purged proteins to a final concentration of 50 mM. CuCl_2 was then added such that the final copper concentration was 25% in excess of the protein concentration. The proteins were dialyzed against 20 mM ACES and 10 mM ascorbate (pH 7.0) to remove unbound copper. The final concentration of protein was determined using the Bradford assay (19) (Bio-Rad). For extended X-ray absorption fine structure (EXAFS) sample preparation, proteins were mixed with 20–30% ethylene glycol, transferred to EXAFS cuvettes, and flash-frozen in liquid nitrogen. The final EXAFS samples were SeM-CusF in apo and Cu(I)-bound forms, at concentrations of 380 and 200 μM , respectively, Cu(I)-SeM-CusF mixed with apo-CusB, and Cu(I)-CusB mixed with apo-SeM-CusF. In the samples containing Cu(I)-SeM-CusF and apo-CusB, the final concentrations of both proteins were 110 μM . To measure different time points, three identical samples of CusF and CusB were prepared, which only differed in the amount of time they were mixed before addition of ethylene glycol and flash-freezing after either 4, 14, or 34 min. For the sample containing Cu(I)-bound CusB and apo-SeM-CusF, the final concentration of apo-SeM-CusF was 85 μM and that of Cu(I)-CusB was 125 μM .

XAS Data Collection and Analysis. Cu K-edge (8.980 keV) and Se K-edge (12.658 keV) EXAFS data for CusF and CusB were collected at the Stanford Synchrotron Radiation Laboratory operating at 3 GeV with currents between 100 and 50 mA. All samples were measured on beamline 9-3 using a Si[220] monochromator and a Rh-coated mirror upstream of the monochromator with a 13 keV (Cu) or 15 keV (Se) energy cutoff to reject harmonics. A second Rh mirror downstream of the monochromator was used to focus the beam. Data were collected in fluorescence mode on a high-count rate Canberra 30-element Ge array detector with maximum count rates below 120 kHz. A Z-1 metal oxide (Ni, As) filter and Soller slit assembly were placed in front of the detector to reduce the elastic scatter peak. Four to six scans of a sample containing only sample buffer [50 mM sodium phosphate (pH 7.2)] were collected at each absorption edge, averaged, and subtracted from the averaged data for the protein samples to remove Z-1 K_β fluorescence and produce a flat pre-edge baseline. This procedure allowed data with an excellent signal-to-noise ratio to be collected down to a total copper concentration of 100 μM in the sample. The samples (80 μL) were measured as aqueous glasses (>20% ethylene glycol) at 10–15 K. Energy calibration was achieved by reference to the first inflection point of a copper metal foil (8980.3 eV) for Cu K-edges and a selenium metal

foil (12658.0 eV) for Se K-edges, placed between the second and third ionization chambers. Data reduction and background subtraction were performed with the program modules of EXAFSPAK [George, G. N. (1990) EXAFSPAK. Stanford Synchrotron Radiation Laboratory, Menlo Park, CA.]. Data from each detector channel were inspected for glitches or drop-outs before inclusion in the final average. Spectral simulation was carried out with EXCURVE 9.2 (20–23) as previously described using 8985 and 12663 eV for the start of the EXAFS in k space ($k = 0$) for Cu and Se EXAFS, respectively (24).

For Se EXAFS analysis of the sample of apo-CusB added to Cu(I)-SeM-CusF, the Se–Cu coordination number was allowed to vary while its DW factor was held constant at 0.005 \AA^2 . Small variations in metrical parameters ($R_{\text{Se-C}}$, $R_{\text{Se-Cu}}$, and $R_{\text{Se-Se}}$) were permitted. The analysis led to excellent fits with a 50% reduction in Se–Cu shell occupancy and a small increase (~ 0.02 \AA) in the Se–Cu bond length, but no difference in Se–C or Se–Se interactions.

RESULTS

Metal-Dependent Interaction of CusF and CusB. To establish whether CusF could play a role as a metallochaperone, we first tested for evidence of an interaction between the two proteins in vitro using isothermal titration calorimetry, a technique that detects the heat absorbed or released during a binding event (i.e., the binding enthalpy change). The titration of Ag(I)-CusF into the solution of apo-CusB (Figure 1A) and the reverse titration of Ag(I)-CusB into apo-CusF (Figure 1B) both showed significant changes in enthalpy. Because the observed enthalpy change could include contributions from both metal binding and protein–protein interactions, no attempt was made to extract binding affinities from the ITC data. An enthalpy change was not observed in the control titrations of Ag(I)-CusF into buffer or buffer into apo-CusB (data not shown). Additionally, no change in the heat absorbed or released was detected upon titration of apo-CusF into apo-CusB (Figure 1a of the Supporting Information), demonstrating that the observed interaction depended on the presence of metal ion. Furthermore, titration of Ag(I)-CusF into Ag(I)-CusB also showed no change in enthalpy (Figure 1b of the Supporting Information), indicating that an enthalpy change for this system requires one of the two proteins to exist in the apo form.

Transfer of Copper between CusF and CusB. If CusF functions as a metallochaperone, it should be able to transfer metal to CusB. To observe direct transfer of metal between the two proteins, a novel X-ray absorption spectroscopy (XAS) technique was developed to follow the copper environment in samples of CusF and CusB. XAS is a spectroscopic technique that provides both electronic structure and atomic-resolution molecular structure information, acting as a bridge between molecular and electronic structure techniques. CusF and CusB both have three-coordinate metal sites, with CusF having two sulfur ligands from methionines and one nitrogen ligand from a histidine (25, 26) and CusB having three sulfur ligands from methionines (16). To distinguish the ligands arising from the methionines of each protein, selenomethionine was incorporated in CusF in place of methionine (SeM-CusF). Extended X-ray absorption fine structure (EXAFS) data at the Se edge were collected for

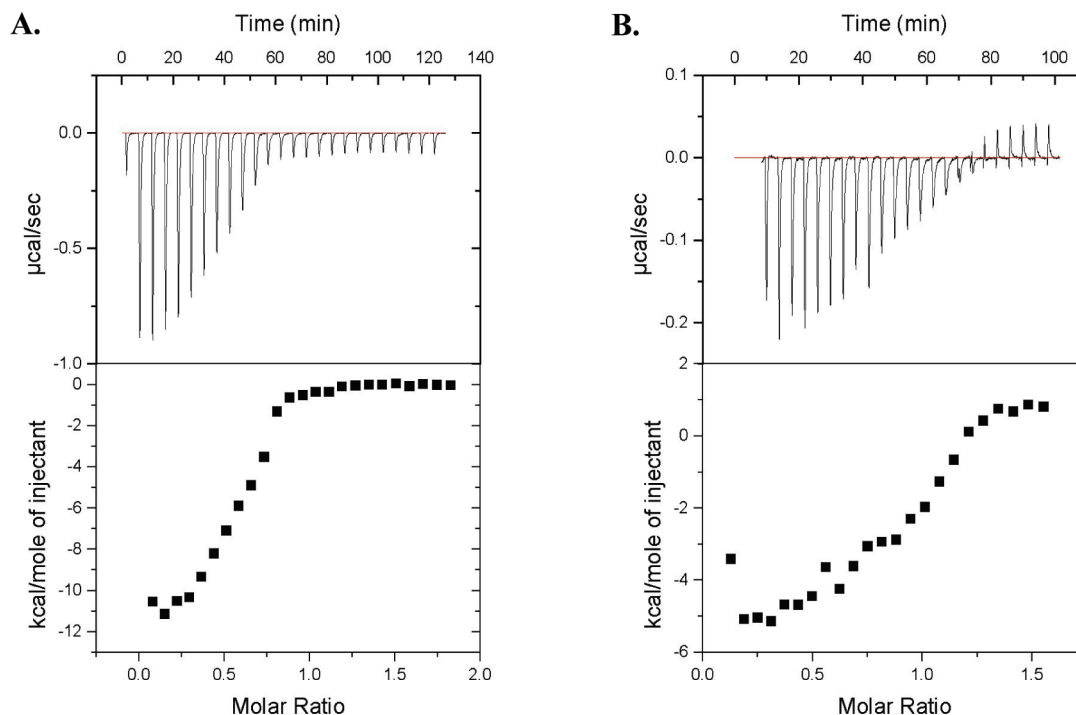


FIGURE 1: Isothermal titration calorimetry of CusF and CusB. (A) Ag(I)-CusF (375 μ M) titrated into apo-CusB (24 μ M). (B) Ag(I)-CusB (142 μ M) titrated into apo-CusF (17 μ M).

Table 1: Obtained Fits to the EXAFS of CusF and CusB by Curve Fitting Using EXCURVE 9.2

	F^a	no. ^c	R (\AA) ^d	DW (\AA^2)	no. ^c	R (\AA) ^d	DW (\AA^2)	no. ^c	R (\AA) ^d	DW (\AA^2)	$-E_0$
Cu edge			C–N(His)^b			Cu–Se			Cu–S		
Cu(I)-CusF	0.364	1	2.01	0.003	2.0	2.41	0.009				4.75
Cu(I)-CusF and apo-CusB											
4 min	0.336	0.48	2.05	0.003	0.96	2.43	0.005	1.57	2.29	0.009	5.07
14 min	0.374	0.62	2.06	0.002	1.24	2.43	0.007	1.14	2.29	0.006	6.98
34 min	0.444	0.49	2.08	0.003	0.99	2.42	0.005	1.52	2.28	0.010	5.32
Se edge			Se–C(Met)			Se–Cu			Se–Se		
apo-CusF	0.518	2.0	1.96	0.004				1.0	2.84	0.036	5.58
Cu(I)-CusF	0.545	2.0	1.96	0.005	0.5	2.41	0.005	1.0	2.85	0.030	5.98
Cu(I)-CusF and apo-CusB											
4 min	0.522	2.0	1.97	0.005	0.30	2.42	0.005	1.0	2.84	0.030	6.13
14 min	0.548	2.0	1.96	0.006	0.26	2.43	0.004	1.0	2.84	0.029	5.62
34 min	0.675	2.0	1.96	0.004	0.29	2.43	0.005	1.0	2.83	0.032	5.62
Cu(I)-CusB and apo-CusF	0.880	2	1.96	0.005	0.3	2.43	0.005	1.0	2.85	0.029	5.98

^a F is a least-squares fitting parameter defined as $F^2 = (1/N) \sum_{i=1}^N k^6(\text{data} - \text{model})^2$. ^b Fits modeled histidine coordination by an imidazole ring, which included single and multiple scattering contributions from the second shell (C2 and C5) and third shell (C3 and N4) atoms, respectively. The Cu–N–Cx angles were as follows: 126° for Cu–N–C2, -126° for Cu–N–C3, 163° for Cu–N–N4, and -163° for Cu–N–C5. ^c Coordination numbers are generally considered to be accurate to $\pm 25\%$. The fractional coordination numbers listed here represent the results obtained from allowing the coordination numbers to vary using the constraints $N_{\text{Cu–N}} = 0.5N_{\text{Cu–Se}}$ and $N_{\text{Cu–S}} = 3 - 1.5N_{\text{Cu–Se}}$ (see the text). While this approach overestimates the accuracy that can be obtained from the simulations, we have retained the two-significant digit format to ensure consistency with the formula for the imposed constraints. ^d In any one fit, the statistical error in bond lengths is ± 0.005 \AA . However, when errors due to imperfect background subtraction, phase-shift calculations, and noise in the data are compounded, the actual error is probably closer to ± 0.02 \AA .

apo-SeM-CusF and Cu(I)-SeM-CusF (Table 1 and Figures 2 and 3 of the Supporting Information). The Fourier transform (FT) spectra show the expected features for the apo and Cu(I)-bound proteins as anticipated from the previous EXAFS characterization of CusF without SeM incorporation (17). The similarity of the Se–Se distance in the apo and Cu(I)-bound proteins implies that the relative positions of the Se atoms in the metal binding site do not change when Cu(I) binds and that the site is therefore preformed for metal binding. The Cu EXAFS data similarly support the structural description of the metal binding site with Cu(I) bound by one His and two SeM ligands (Table 1 and Figure 4 of the Supporting Information).

The addition of apo-CusB to a Cu(I)-SeM-CusF sample caused significant changes in the Se and Cu EXAFS spectra

(Figure 5 of the Supporting Information). The most dramatic effects are seen in the FT of the Se EXAFS, where a significant decrease in the intensity of the Se–Cu peak is observed, while the intensity of the Se–C peak (Figure 2A) remains unchanged. The Se–C interaction derives from the methyl and methylene carbons from the methionine side chain and thus acts as an internal standard for comparing intensities of Fourier transforms. Since CusF, but not CusB, is labeled with Se, the decrease in the Se–Cu bond length measured by Se EXAFS is the result of loss of Cu(I) specifically from the CusF binding site. Spectral fitting showed transfer of $\sim 50\%$ of the Cu(I) out of the Se environment. This distribution likely reflects the similar affinities of CusF and CusB for metal (16, 27). These results demonstrate the unique strength of SeM substitution coupled

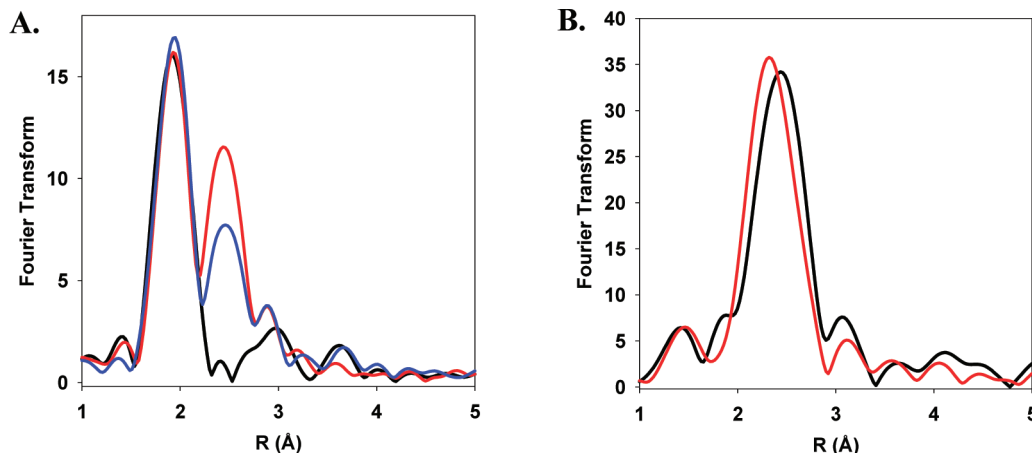


FIGURE 2: EXAFS data of SeM-CusF and CusB mixtures. (A) Comparison of the Fourier transforms of EXAFS data measured at the Se edge of Cu(I)-SeM-CusF (red), Cu(I)-SeM-CusF mixed with apo-CusB for 34 min before freezing (blue), and apo-SeM-CusF (black). (B) Comparison of the Fourier transforms of EXAFS data measured at the Cu edge of Cu(I)-SeM-CusF (black) and Cu(I)-SeM-CusF mixed with apo-CusB for 34 min before freezing (red).

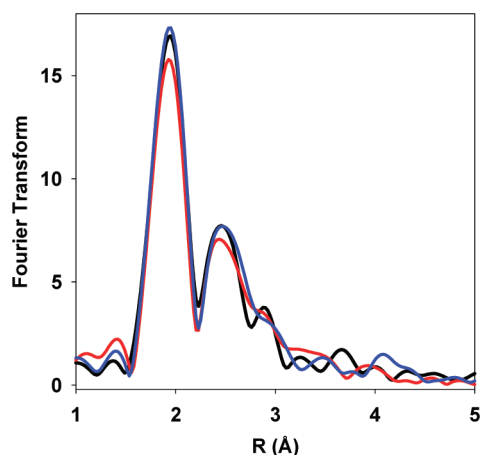


FIGURE 3: Comparison of the Fourier transforms of EXAFS data measured at the Se edge for samples of Cu(I)-SeM-CusF mixed with apo-CusB for different times before freezing: 4 min (black), 14 min (red), and 34 min (blue).

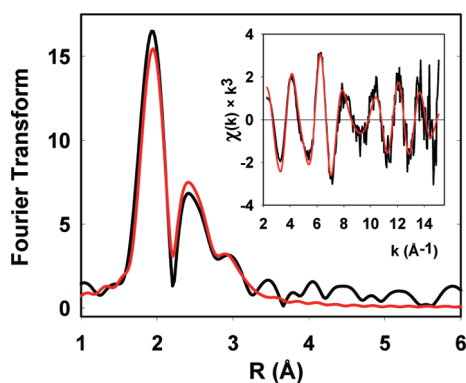


FIGURE 4: EXAFS data of Cu(I)-CusB mixed with apo-SeM-CusF measured at the Se edge. Experimental (black traces) vs simulated (red traces) FT and EXAFS (inset) using metrical parameters listed in Table 1.

to Se-XAS analysis as a ligand-directed monitor of metal transfer reactions.

Analysis of the Cu EXAFS provided an additional probe of metal transfer. In previous work, we reported that CusB binds Cu(I) in an all-S environment, with coordination to three methionine residues with Cu–S bond lengths of 2.28–2.30 Å (16). Transfer of copper from CusF to CusB

should therefore be accompanied by loss of Cu–N and Cu–Se bonds (the ligands to CusF) and replacement by the Cu–S (Met) environment of CusB. Knowledge of the binding site environment of both donor and acceptor protein allowed us to set constraints on the coordination numbers $N_{\text{Cu-N}}$ and $N_{\text{Cu-S}}$ as follows:

$$N_{\text{Cu-N}} = 0.5N_{\text{Cu-Se}}$$

$$N_{\text{Cu-S}} = 3 - 1.5N_{\text{Cu-Se}}$$

The data were analyzed by imposing these constraints and allowing only the Cu–Se coordination number, $N_{\text{Cu-Se}}$, to vary, with small variations in distances permitted. The result of these simulations is that the Cu–Se coordination number dropped by 50%, exactly equivalent to the change observed at the Se edge, while an appropriate increase in Cu–S shell occupancy at $R = 2.29$ Å was observed (Table 1). The FT of the Cu EXAFS data is shown in Figure 2B. While not as easily detectable as the changes observed at the Se edge, transfer from CusF to CusB is evident from the shift in the main transform peak to a lower R value, as the Cu transfers out of the Cu–Se ($R = 2.4$ Å) environment of CusF into the Cu–S ($R = 2.3$ Å) environment of CusB. The Cu EXAFS data are thus consistent with 50% Cu(I) transfer into the all-S environment of the CusB protein, with a Cu–S distance equal to that obtained previously from studies on the fully reconstituted Cu(I)-CusB protein (16).

In addition to the sample described above, which was incubated for 34 min before being frozen, two additional samples, incubated for 4 and 14 min before being frozen, were made. In both cases, the extent of transfer was close to 50% and the Se data were identical to those of the 34 min sample (Figure 3, Table 1, and Figure 5 of the Supporting Information). This result indicates that metal transfer is relatively rapid and proceeds to an end point of equal Cu(I) distribution between donor and acceptor in less than 4 min (the time taken to mix and freeze the solution).

To examine whether metal transfer can directly occur in the opposite direction from CusB to CusF, we monitored the Cu and Se EXAFS of a sample of Cu(I)-CusB mixed with apo-CusF. The spectra show the loss of the Cu(I)–S environment of CusB and replacement by the Cu(I)–Se

environment of SeM-CusF (Figure 4). Again, Cu(I) shows an approximately 50% distribution between the CusB and CusF proteins. Therefore, transfer of Cu(I) between CusF and CusB is reversible and proceeds to an equivalent end point regardless of which protein is preloaded with Cu(I).

Interaction and Metal Transfer between CusF and CusB Are Specific. To confirm that metal is directly transferred between CusF and CusB, not released into solution and rebound by the proteins, we performed ITC experiments with a homologue of CusF, SilF, which is 51% identical in sequence to CusF and binds Ag(I) with similar affinity ($K_d = 35$ nM) (Figure 6a of the Supporting Information). The titrations of both Ag(I)-CusF into apo-SilF and Ag(I)-SilF into apo-CusF show no significant enthalpy changes (Figure 6b,c of the Supporting Information), indicating no metal transfer between these proteins.

Importantly, we determined that the homologue of CusF, SilF, is unable to productively interact with CusB. Using ITC, no enthalpy changes are observed during the course of a titration of Ag(I)-SilF into apo-CusB (Figure 6d of the Supporting Information). This result implies that specific recognition is required for the metal transfer event and that metal transfer is direct between proteins of the Cus system. This high degree of specificity in the transfer process may serve as a protective mechanism to ensure that metals remain sequestered among the Cus proteins and help prevent the toxic effects of free copper or silver.

DISCUSSION

Our results demonstrate a role for CusF as a periplasmic metallochaperone for a copper efflux system. Through isothermal titration calorimetry experiments, we have demonstrated that interactions occur only between CusF and CusB in the presence of metal. A close homologue of CusF is unable to interact with or transfer metal to CusB, thus demonstrating a high degree of specificity in the interaction. Using selenomethionine-labeled protein to distinguish the metals sites of the two proteins in XAS experiments, we were able to unequivocally show the direct transfer of Cu(I) from one protein to the other. Periplasmic metallochaperones, in analogy to eukaryotic metallochaperones, play a dual protective role within the cell. Via sequestration of metal within the confines of a protein, coupled with specific transfer to a target protein, the cytotoxic effects of the free metal can be avoided.

CusF may provide specificity for monovalent metal resistance systems that is lacking in other RND- or CBA-type exporters. The homologous multidrug resistance systems, which lack an equivalent of CusF, have very broad substrate specificity, leading to their description as "periplasmic vacuum cleaners" (28). In addition to the sequestration and delivery function implied by the identification of CusF as a metallochaperone, the CusF protein may play a role in specific substrate selection, so it does not remove needed metals from the cell.

We have shown that metal transfer occurs in both directions between CusF and CusB and proceeds to a 50% equilibrium distribution in vitro. In light of these findings, how could CusF effectively function as a metallochaperone? Because the affinities of the individual proteins are similar, in a system where only the two purified compo-

nents are present at equilibrium the metal is expected to partition equally between the two proteins, as we have experimentally observed. This shallow thermodynamic gradient is similar to what has been previously reported for a yeast copper chaperone and the regulatory domain of a copper-transporting ATPase (29). In the case of the Cus system, in the cell where the complete efflux complex is present and where energy from the proton gradient can be utilized to drive transport, our model is one in which metal will be continually removed from CusB and therefore unidirectional transfer of metal from CusF to CusB will occur, even in the case of a shallow thermodynamic gradient. Consistent with this, in another system where the transport site is present, transfer from the chaperone to an ATPase is essentially irreversible (30). In this model, CusF could efficiently function as a metallochaperone, though both proteins have similar binding affinities for metal and metal transfer can occur in both directions.

The site of entry of metal into the efflux complex is not yet known; however, metal transfer from CusF to CusB provides evidence of entry of substrates from the periplasm into the RND efflux system. In homologous multidrug resistance systems, evidence suggests that the substrates are bound by the periplasmic domains of inner membrane proteins (14, 15, 31), with no substrate binding function by the periplasmic component equivalent to CusB. For hydrophobic substrates dissolved in the inner membrane, this pathway would make sense. Though at this point a regulatory role for metal binding by CusB cannot be ruled out, in the metal efflux system the substrates are likely to be entering the complex from the aqueous periplasmic space, and thus, the transfer of metal from CusF to CusB may be the direct point of entry for the transport system.

SUPPORTING INFORMATION AVAILABLE

Supplementary Figures 1–6. This material is available free of charge via the Internet at <http://pubs.acs.org>.

REFERENCES

1. Nelson, N. (1999) Metal ion transporters and homeostasis. *EMBO J.* 18, 4361–4371.
2. Wong, M. D., Fan, B., and Rosen, B. P. (2004) *Handbook of ATPases: Biochemistry, Cell Biology, Pathophysiology*, Wiley-VCH: Weinheim, Germany.
3. Singleton, C., and Le Brun, N. E. (2007) Atx1-like chaperones and their cognate P-type ATPases: Copper binding and transfer. *BioMetals* 20, 275–289.
4. Poulos, T. L. (1999) Helping copper find a home. *Nat. Struct. Biol.* 6, 709–711.
5. Culotta, V. C., Lin, S. J., Schmidt, P., Klomp, L. W. J., Casareno, R. L. B., and Gitlin, J. (1999) Intracellular pathways of copper trafficking in yeast and humans. *Adv. Exp. Med. Biol.* 448, 247–254.
6. O'Halloran, T. V., and Culotta, V. C. (2000) Metallochaperones, an intracellular shuttle service for metal ions. *J. Biol. Chem.* 275, 25057–25060.
7. Rosenzweig, A. C. (2001) Copper delivery by metallochaperone proteins. *Acc. Chem. Res.* 34, 119–128.
8. Finney, L. A., and O'Halloran, T. V. (2003) Transition metal speciation in the cell: Insights from the chemistry of metal ion receptors. *Science* 300, 931–936.
9. Culotta, V. C., Yang, M., and O'Halloran, T. V. (2006) Activation of superoxide dismutases: Putting the metal to the pedal. *Biochim. Biophys. Acta* 1763, 747–758.

10. Cobine, P. A., Piefffel, F., and Winge, D. R. (2006) Copper trafficking to the mitochondrion and assembly of copper metalloenzymes. *Biochim. Biophys. Acta* 1763, 759–772.
11. Macomber, L., Rensing, C., and Imlay, J. A. (2007) Intracellular copper does not catalyze the formation of oxidative DNA damage in *Escherichia coli*. *J. Bacteriol.* 189, 1616–1626.
12. Franke, S., Grass, G., Rensing, C., and Nies, D. H. (2003) Molecular analysis of the copper-transporting efflux system CusCFBA of *Escherichia coli*. *J. Bacteriol.* 185, 3804–3812.
13. Tseng, T. T., Gratwick, K. S., Kollman, J., Park, D., Nies, D. H., Goffeau, A., and Saier, M. H., Jr. (1999) The RND permease superfamily: An ancient, ubiquitous and diverse family that includes human disease and development proteins. *J. Mol. Microbiol. Biotechnol.* 1, 107–125.
14. Murakami, S., Nakashima, R., Yamashita, E., Matsumoto, T., and Yamaguchi, A. (2006) Crystal structures of a multidrug transporter reveal a functionally rotating mechanism. *Nature* 443, 173–179.
15. Seeger, M. A., Schiefner, A., Eicher, T., Verrey, F., Diederichs, K., and Pos, K. M. (2006) Structural asymmetry of AcrB trimer suggests a peristaltic pump mechanism. *Science* 313, 1295–1298.
16. Bagai, I., Liu, W., Rensing, C., Blackburn, N. J., and McEvoy, M. M. (2007) Substrate-linked conformational change in the periplasmic component of a Cu(I)/Ag(I) efflux system. *J. Biol. Chem.* 282, 35695–35702.
17. Loftin, I. R., Franke, S., Roberts, S. A., Weichsel, A., Heroux, A., Montfort, W. R., Rensing, C., and McEvoy, M. M. (2005) A novel copper-binding fold for the periplasmic copper resistance protein CusF. *Biochemistry* 44, 10533–10540.
18. Doublet, S. (1997) Preparation of selenomethionyl proteins for phase determination. *Methods Enzymol.* 276, 523–530.
19. Bradford, M. M. (1976) Rapid and sensitive method for quantitation of microgram quantities of protein utilizing principle of protein-dye binding. *Anal. Biochem.* 72, 248–254.
20. Gurman, S. J., Binsted, N., and Ross, I. (1984) A rapid, exact, curved-wave theory for EXAFS calculations. *J. Chem. Phys.* 17, 143–151.
21. Gurman, S. J., Binsted, N., and Ross, I. (1986) A rapid, exact, curved-wave theory for EXAFS calculations. II. The multiple-scattering contributions. *J. Chem. Phys.* 19, 1845–1861.
22. Binsted, N., Gurman, S. J., and Campbell, J. W. (1998) EXCURVE 9.2, Daresbury Laboratory, Warrington, England.
23. Binsted, N., and Hasnain, S. S. (1996) State-of-the-art analysis of whole X-ray absorption spectra. *J. Synchrotron Radiat.* 3, 185–196.
24. Blackburn, N. J., Ralle, M., Hassett, R., and Kosman, D. J. (2000) Spectroscopic analysis of the trinuclear cluster in the Fet3 protein from yeast, a multinuclear copper oxidase. *Biochemistry* 39, 2316–2324.
25. Loftin, I. R., Franke, S., Blackburn, N. J., and McEvoy, M. M. (2007) Unusual Cu(I)/Ag(I) coordination of *Escherichia coli* CusF as revealed by atomic resolution crystallography and X-ray absorption spectroscopy. *Protein Sci.* 16, 2287–2293.
26. Xue, Y., Davis, A. V., Balakrishnan, G., Stasser, J. P., Staehlin, B. M., Focia, P., Spiro, T. G., Penner-Hahn, J. E., and O'Halloran, T. V. (2008) Cu(I) recognition via cation- π and methionine interactions in CusF. *Nat. Chem. Biol.* 4, 107–109.
27. Kittleson, J. T., Loftin, I. R., Hausrath, A. C., Engelhardt, K. P., Rensing, C., and McEvoy, M. M. (2006) Periplasmic metal-resistance protein CusF exhibits high affinity and specificity for both Cu-I and Ag-I. *Biochemistry* 45, 11096–11102.
28. Lomovskaya, O., Zgurskaya, H. I., Totrov, M., and Watkins, W. J. (2007) Waltzing transporters and 'the dance macabre' between humans and bacteria. *Nat. Rev. Drug Discovery* 6, 56–65.
29. Huffman, D. L., and O'Halloran, T. V. (2000) Energetics of copper trafficking between the Atx1 metallochaperone and the intracellular copper transporter, Ccc2. *J. Biol. Chem.* 275, 18611–18614.
30. Gonzalez-Guerrero, M., and Arguello, J. M. (2008) Mechanism of Cu⁺-transporting ATPases: Soluble Cu⁺ chaperones directly transfer Cu⁺ to transmembrane transport sites. *Proc. Natl. Acad. Sci. U.S.A.* 105, 5992–5997.
31. Yu, E. W., Aires, J. R., McDermott, G., and Nikaido, H. (2005) A periplasmic drug-binding site of the AcrB multidrug efflux pump: A crystallographic and site-directed mutagenesis study. *J. Bacteriol.* 187, 6804–6815.

BI801638M